THE ASTROPHYSICAL JOURNAL, 247:569–576, 1981 July 15

MULTISLIT PHOTOELECTRIC MAGNETOMETER OBSERVATIONS OF CEPHEIDS AND SUPERGIANTS: PROBABLE DETECTIONS OF WEAK MAGNETIC FIELDS

ERMANNO F. BORRA
Département de Physique, Observatoire du Mont Mégantic, Université Laval
AND
J. M. FLETCHER AND R. POECKERT
Dominion Astrophysical Observatory
Received 1980 November 24; accepted 1981 January 30

ABSTRACT

We have assembled an instrument that measures the circular polarization in 230 spectral lines simultaneously. The instrument is capable of measuring longitudinal magnetic fields in bright stars with standard deviations of the order of 1 gauss. We have obtained several detections at the 2, 3, and up to 4.6 standard deviations level in the Cepheid variables α UMi and δ Cep and in the F8 Ib supergiant γ Cyg, indicating longitudinal fields from 10 to 30 gauss. A thorough error analysis shows that we did not underestimate our errors and that the detections are very likely to be real. Other Cepheids observed with lower precision ($\sigma \sim 40$ gauss) do not give significant detections. It would thus appear that Cepheids as a class have magnetic fields with longitudinal components of a few tens of gauss. Our observations thus lend support to the hypothesis advanced by Stothers to reconcile pulsational and evolutionary masses. As a check on the technique, we have also observed the known magnetic star β CrB, obtaining very high signal-to-noise ratio measurements that define a remarkably sinusoidal magnetic curve indicative of a dominant dipolar component.

Subject headings: instruments — stars: Cepheids — stars: magnetic — stars: supergiants — Zeeman effect

I. INTRODUCTION

Photoelectric techniques have been used for some time now (Babcock 1953) to measure weak magnetic fields in the Sun, and they have proved to be capable of detecting very small magnetic fields (Howard 1977). Variations on the basic Babcock technique have also been used more recently to measure stellar magnetic fields. However, the formal errors are fairly large, usually of the order of 100 gauss (Borra and Landstreet 1973, 1980). All the photoelectric magnetic stellar observations have measured only one spectral line at a time, and, therefore, a considerable increase in precision could readily be attained by observing the circular polarization in several spectral lines simultaneously. This increase in precision is desirable in relation to several astrophysical problems.

Recently, there has been renewed interest in the magnetism of pulsating variables. Weiss and Wood (1975), Wood, Weiss, and Jenkner (1977), and Weiss, Dorfi, and Tscharnuter (1980) have observed photographically several classical Cepheids, reporting the presence of variable magnetic fields. Stothers (1979) has studied theoretically the effect that a magnetic field has on the pulsational behavior of a classical Cepheid. He finds that the known discrepancy between the pulsational and evolutionary theoretical masses of classical Cepheids can be reconciled if the effects of a magnetic field are taken into account in determining pulsational masses.

We have carried out a search for longitudinal magnetic fields in several classical Cepheids, using a multislit photoelectric magnetometer capable of attaining precision an order of magnitude better than previous instruments.

II. THE TECHNIQUE

We have improved the technique used by Borra and Landstreet (1973) by using a template with several slits matching the stellar spectrum, instead of a unique slit and one line, thus observing the circular polarization in about 230 lines simultaneously. We have accomplished this by interfacing the optics and electronics of the Laval University Pockels cell polarimeter with the radial velocity spectrometer attached to the 9682M (2.4 Å mm^{-1}) coudé spectrograph of the Dominion Astrophysical Observatory (DAO) 1.2 m telescope. This radial velocity spectrometer is similar to the Palomar 5 m spectrometer described by Griffin and Gunn (1974), with some modifications, as described by McClure, Fletcher, and Nemec (1980).

A KD* P crystal, followed by a Glan-Thompson prism, is placed in front of the entrance slit of the spectrograph. The crystal is modulated $\pm\lambda/4$ with high-voltage square pulses at a frequency of 100 Hz. In conjunction with a Glan-Thompson prism, this results in, alternately, the left and the right circularly polarized components of the starlight being admitted into the spectrograph (at 100 Hz). For a more detailed and technical discussion of this technique applied to the measurements of stellar magnetic fields, see Borra (1981). The advantage of this technique comes from the fact that the net polarization is measured as a difference in intensity between two otherwise identical beams, separated in time by 10 milliseconds, with the same detector.

We first use the instrument in its radial-velocity measuring mode and find the position at which the mask matches the stellar spectrum. The mask is then positioned so that the slits admit the light from the blue wings of the stellar spectral lines. The photon counts from the photomultiplier and preamplifier are then routed to the photon-counting electronics of the polarimeter, and the circular polarization is then measured (switching at 100 Hz) during a fixed period of time (typically 5 minutes), after which the circular polarization signal V_b^1 is recorded. The slits are then moved to the opposite (red) wings of the lines, and the polarization is measured for an equal length of time, yielding V_r^1. The sequence continues in the order $V_b^1, V_r^1, V_r^2, \ldots V_b^{n-1}, V_b^n, V_r^n$, giving after n pairs of integrations:

$$\langle V \rangle = \sum_{i=1}^{n} \frac{V_r^i - V_b^i}{2n}. \quad (1)$$

This sequence is chosen to minimize the effects of the time-varying instrumental polarization.

Oblique reflections off metallic mirrors introduce spurious polarization and phase shifts which cause depolarization of a stellar signal and cross-talk among the Stokes parameters (Borra 1976). The configuration of the DAO 48 inch (1.2 m) coudé is the same as the configuration of the five-mirror system discussed by Borra (1976), where it can be seen that the instrumental effects are large (for aluminized mirrors) and complex because they vary with declination and hour angle. For a given star, the instrumental polarization is thus a function of time $P(t)$. It can be shown, by doing a series expansion of $P(t)$, that the chosen sequence, $\ldots V_b^i, V_r^i, V_r^{i+1}, V_b^{i+1} \ldots$, and equation (1) eliminate the constant and first-order term (dP/dt) in the expansion. Plots of the instrumental polarization measured show that these two terms dominate for our observations. The flat mirrors of the 48 inch (1.2 m) coudé are coated for high reflectance (Richardson, Breakley, and Dancey 1971). Therefore, they are not expected to behave like aluminized mirrors. We checked the depolarization introduced by the whole coudé system by placing a lamp, followed by a diffuser and an HNCP37 circular polarizer, in front of the first flat mirror. The primary and secondary mirrors give nearly normal reflection and, hence, can be neglected. We then measured the circular polarization at the slit area with the polarimeter plus radial-velocity meter in their usual "stellar" mode of operation. The measurements were repeated at declinations and hour angles covering the whole sky. We found, to our dismay, that the all-dielectrically coated mirrors usually used in the blue region of the spectrum are unsuited for polarization measurements as they depolarized catastrophically the HNCP37 signal. We then checked, in the same fashion, the coated silver mirrors that are usually used in the red. In the wavelength region we used (4500 ± 175 Å), they have only slightly smaller reflectivity than the all-dielectric mirrors. Happily, these mirrors are eminently well suited for polarization measurements as they introduce very little instrumental polarization and negligible depolarization. We therefore did not use a phase shift compensator during our observations. The small instrumental polarization [$P(t) \leq 0.2\%$] is removed in large measure by equation (1).

III. CALIBRATION AND OBSERVATIONS OF KNOWN MAGNETIC STARS

It can be shown, with a series expansion of the line profile truncated after the first-power term, that for a spectral line having intensity profile $I(\lambda)$, a central wavelength λ (Å), a z-factor z (Babcock 1962), and which is formed in the presence of a homogeneous magnetic field of strength B (gauss) with its lines of force inclined at an angle γ with respect to the line of sight, the fractional circular polarization V is related to the magnetic field strength via the relation:

$$V = 4.67\ 10^{-13} z B \cos\gamma \frac{1}{I}\frac{dI}{d\lambda}\lambda^2. \quad (2)$$

In a real star, the magnetic field is not homogeneous, but numerical models (Borra 1972) show that this relation still holds to good approximation provided $B\cos\gamma$ is replaced with B_e defined as:

$$B_e = \frac{\int |B| \cos\gamma I\, dA}{\int I\, dA}, \quad (3)$$

where the surface integrals are carried over the visible disk of the star, I is the local surface brightness, and dA is the surface area element.

For our observations we use a mask that matches the spectrum of Procyon (F5 IV), is centered at 4500 Å, and

TABLE 1

OBSERVATIONS OF MAGNETIC Ap STARS

JD 2,444,000+	$\langle V \rangle \pm \sigma$ (%)	$B_e \pm \sigma$ (gauss)	ϕ	B_e expected (gauss)
		β Coronae Borealis		
316.882	1.151±0.037	745±24	0.296	650
316.970	1.160±0.036	754±23	0.301	650
408.741	1.049±0.021	682±14	0.265	640
410.730	0.912±0.014	593±9	0.373	590
442.707	0.642±0.015	417±10	0.102	290
444.722	1.030±0.017	670±11	0.212	580
470.698	−0.118±0.040	−77±26	0.617	−120
471.696	−0.438±0.025	−285±16	0.671	−270
472.692	−0.556±0.023	−361±15	0.725	−380
473.685	−0.544±0.023	−354±15	0.778	−430
506.670	−0.044±0.022	−29±14	0.562	60
507.678	−0.273±0.019	−177±12	0.617	−120
508.647	−0.521±0.028	−339±18	0.669	−260
		78 Virginis		
316.936	−0.94 ±0.06	−846±54	0.401	−810

contains 230 slits, each 0.12 Å wide. To convert the polarization signals observed into magnetic fields, we use equations (1) and (2). The value of $1/I(dI/d\lambda)$ used is taken from the cross-correlation profile obtained by the radial-velocity meter because it can be assumed to represent the average line observed. The value of z used is an average z-value that is obtained by averaging z-values in the list of Babcock (1962) and in pages chosen at random in Sylvia Burd's extensive list of z values (unpublished). The average z-value used is 1.3.

To insure ourselves of the basic soundness of our calibration and as a check on the instrument, we observed every night the well-known magnetic Ap star β CrB; our mask is a reasonable match to its metal spectrum (F2). The magnetic B_e curve of the star has been obtained photographically by Wolff and Wolff (1970) and Wolff and Bonsack (1972) and photoelectrically (but with two different techniques also differing from the present one) by Borra and Vaughan (1977) and Borra and Landstreet (1980). These B_e curves are all in basic agreement with each other, but the one obtained by Borra and Landstreet (1980) is probably the most reliable as it was derived from wide-band photoelectric observations in Hβ. As an additional check, we have observed once the magnetic Ap star 78 Vir, which was also observed by Borra and Landstreet (1980). Our observations of magnetic Ap stars are shown in Table 1, where we give the Julian Date at the mid-point of observation, the measured $\langle V \rangle$ value and its standard deviation, the B_e values (and standard deviations) obtained from equation (2), the phases obtained from the ephemerides in Borra and Landstreet (1980), and the B_e values expected at those phases from Borra and Landstreet (1980). Our standard deviations are obtained under the assumption that photon shot noise is the only source of random error. Extensive use of this type of polarimeter shows that this is very nearly the case. The $1/I(dI/d\lambda)$ values used have an uncertainty of about 10–20%, and, therefore, the calibration of our B_e values has the same uncertainty. However, notice that this is only a calibration uncertainty and that the signal-to-noise ratios stay the same as for the polarization values. We can see an excellent agreement between the observed and the computed values, especially if we consider that the least-squares fit in Borra and Landstreet (1980) has an uncertainty of about 50 gauss in amplitude and 0.01 in phase. The agreement is also good for our lone observation of 78 Vir. This illustrates the basic soundness of our calibration procedure, as the spectrum of 78 Vir (A2p) is fairly remote from Procyon's (F5 IV). Our magnetic B_e curve of β CrB is plotted in Figure 1 along with a least-squares fitted sine curve (*solid line*) and the least-squares fitted sine curve from Borra and Landstreet (1980) (*broken line*). The curve from Borra and Landstreet (1980) has been shifted by −0.02 cycles in phase to make the extrema coincide. This shift is compatible with the error in phase (0.0101) quoted by Borra and Landstreet (1980). The error bars ($\pm \sigma$) associated with every observation are shown in Figure 1. Once again, we can see an excellent agreement. The extent to which the sine curve fits the observations is amazing ($\chi^2/\nu = 4.94$, $\nu = 13$), especially in view of the fact that we did not take special precautions to obtain accurate values; for example, the major part of the relatively large value of χ^2/ν is probably due to the positioning of the slits on the line wings (done by eye estimate on the

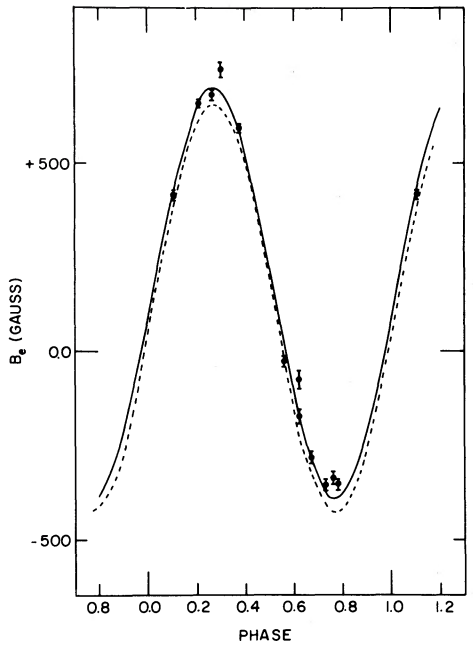

FIG. 1.—The B_e curve of β CrB. The error bars represent 2 standard deviations ($\pm \sigma$). *Solid line*, a least-squares fitted sine curve; *broken line*, the B_e curve of β CrB from Borra and Landstreet (1980).

oscilloscope display). At a 50-to-1 signal-to-noise ratio, also, one should expect systematic errors to come into play. Departures from a dipolar geometry probably contribute also to increase the χ^2/ν value. Figure 1 illustrates the potentials of this technique, showing it to be an apparently feasible method for obtaining extremely accurate B_e curves for bright, sharp-lines, magnetic Ap stars. A typical integration time for a point in Figure 1 is 30 minutes. The magnetic geometries of these stars could thus be modeled accurately by multipole analyses. Hydromagnetic fluctuations on the surfaces of these stars or secular variations could also be detected. The fact that the B_e curve of β CrB is so well fitted by a sine curve (unlike the photographic curves) indicates that its dipolar component dominates and is in agreement with the effects proposed by Borra (1974).

IV. OBSERVATIONS OF CLASSICAL CEPHEIDS AND γ CYGNI

Our observations of classical Cepheids are shown in Table 2, where we give the name of the star, the Julian Date at the mid-point of observation, $\langle V \rangle$ (defined by equation [1]) and its associated standard deviation, B_e (in gauss) and standard deviation from equation (2), and finally the phase from the light-curve ephemeris. The

TABLE 2

OBSERVATIONS OF CLASSICAL CEPHEIDS AND γ CYGNI

Star	JD 2,444,000+	$\langle V \rangle \pm \sigma$ (%)	$B_e \pm \sigma$ (gauss)	ϕ	Remarks
η Aql	408.890	0.024±0.0139	16±9	0.907	...
η Aql	409.931	0.008±0.0130	5±8	0.052	...
η Aql	442.767	−0.002±0.035	−1±23	0.627	...
η Aql	470.789	0.023±0.024	15±16	0.532	...
δ Cep	410.789	−0.004±0.020	−2±8	0.264	...
δ Cep	444.950	−0.039±0.021	−16±8	0.630	1.9 σ
δ Cep	470.893	−0.006±0.021	−2±8	0.464	...
δ Cep	472.995	−0.085±0.030	−34±12	0.856	2.8 σ; Fig. 2; Table 4
δ Cep	473.754	−0.026±0.011	−10.4±4.4	0.997	2.4 σ; Table 4
δ Cep	508.870	0.002±0.031	1±12	0.541	...
γ Cyg	444.775	0.000±0.010	0±6.3	...	Table 4
γ Cyg	471.849	−0.029±0.009	−18.3±5.7	...	3.2 σ; Fig. 2; Table 4
γ Cyg	472.902	−0.015±0.0064	−9.5±4.0	...	2.3 σ; Fig. 2; Table 4
ζ Gem	506.988	−0.014±0.019	−5±7	0.311	...
ζ Gem	509.007	0.043±0.050	16±19	0.566	...
α UMi	408.812	−0.0104±0.0064	−5.2±3.2	0.814	Table 4
α UMi	442.829	−0.014±0.0084	−7.0±4.2	0.383	Table 4
α UMi	444.837	0.031±0.0067	15.5±3.4	0.889	4.6 σ; Fig. 2; Table 4
α UMi	470.984	−0.005±0.0065	−2.5±3.2	0.475	Table 4
α UMi	471.744	−0.007±0.0096	−3.5±4.8	0.667	Table 4
α UMi	472.770	−0.013±0.0057	−6.5±2.9	0.925	2.3 σ; Fig. 2, Table 4
α UMi	473.861	−0.014±0.0067	−7.0±3.4	0.200	2.1 σ; Table 4
FF Aql	506.734	0.038±0.043	21±24	0.408	...
RT Aur ...	507.972	0.053±0.057	33±35	0.802	...
SU Cas ...	507.828	0.014±0.044	14±44	0.207	...
DT Cyg ...	506.818	0.048±0.042	31±27	0.830	...
X Cyg	508.717	−0.022±0.28	−10±120	0.380	...
S Sge	507.745	0.001±0.037	0±16	0.980	...

TABLE 3

MEASUREMENTS OF NULL STANDARDS

Star	JD (2,444,000+)	$\langle V \rangle \pm \sigma$ (%)
α Lyr ...	344.042	0.001 ± 0.006
α Lyr ...	507.638	0.0005 ± 0.003
α Aur ...	506.915	0.002 ± 0.004

ephemerides are obtained from Schaltenbrand and Tammann (1971). We have obtained several observations of the brightest Cepheids visible from the northern hemisphere. These most precise measurements are listed first in Table 2. We have also included, in this short list, the F8 Ib star γ Cyg, which has been reported to be magnetic (Severny 1970; Borra and Landstreet 1973). We can see several detections at the 2, 3, and even 4 standard deviations level. A 3 standard deviations detection is usually taken to be at the borderline of a definite detection; therefore, on the basis of Table 3, we would have to conclude that we have discovered magnetic fields in those stars. We have also observed several fainter Cepheids, and, where we can see that we do not obtain a significant signal with these lower precision measurements, we have listed the observations at the end of Table 2. We would therefore have to conclude that Cepheids, as a class, have weak magnetic fields that usually have longitudinal components of the order of a few tens of gauss.

Because the errors in the first part of Table 2 are by far the smallest ever claimed for magnetic observations of stars, it is legitimate to wonder whether Table 2 is a statement about the limits of the technique rather than about the presence of magnetic fields in Cepheids. In other words, are our errors realistic? Measurements of greater precision to confirm our detections will be difficult to obtain, as it will take a major effort and the construction of a more complex and specialized instrument, on a large telescope, to decrease our errors by as much as a factor of 2. It is therefore worthwhile to discuss our observations in detail. It is important to understand that our instrument is, first of all, a polarimeter which, as such, measures a circular polarization signal which is then converted in gauss with equation (2) to yield an astrophysically meaningful number. However, in a discussion concerning experimental errors, it is more appropriate to compare polarization signals. The Pockels cell technique is clearly capable of measuring polarization signals at the 0.010% level, as many of the measurements reported by Borra and Landstreet (1980), determined with the same type of optics and electronics, had errors as low as 0.004%. However, in our case, we are working at the coudé focus, so that one might wonder whether inadequate subtraction of time-varying instrumental polarization, or other unknown causes, might not give spurious detections. We have enough null measurements with $\sigma > 0.010\%$ that one does not have to worry about measurements having $\sigma > 0.010\%$. Doubts might instead be raised about our more precise measurements. We have therefore made a detailed error analysis of our observations having $\sigma < 0.010\%$. We have also observed what is essentially a continuum source (Vega, A0 V) for our mask and one bright G8 star (α Aur). We can see null detections (Table 3) for those two objects. Because obtaining these null measurements is just as time consuming (and less rewarding) than obtaining other observations, we did not pursue a vigorous program of null observations. We decided against it as well because, first, Table 3 shows that the instrument is capable of measures of less than 0.010% and, second, an error analysis can be carried out solely from the observations listed in Table 2. Every entry in Tables 1, 2, and 3 is an average (eq. [1]) of $2n$ individual observations (usually 10–20) that should scatter at random around the instrumental polarization line for null measurement and around $\langle V \rangle$ for positive detections. We have plotted in Figure 2 the raw polarization measurements, as a function of hour angle+constant, of our highest signal-to-noise ratio detections in Table 2 and our null measurements in Table 3. The observations are identified by the name of the star and the Julian Date ($-2{,}444{,}000.00$). The filled circles show observations on the blue wings of the spectral lines, and the open circles show observations on the red wings. The straight lines in Figure 2 show least-squares–fitted instrumental polarization lines with

$$P(t) = a + bt. \tag{4}$$

The error bars associated with every individual measurement are shown for a few points and represent 2 standard deviations ($\pm \sigma$). They are obtained under the assumption that photon noise is the only source of random error. We can see, for our detections, that the observations on the blue wings tend to lie on one side of $P(t)$, while our null measurements scatter at random. This behavior is typical of our observations listed in Tables 3 and 4 and shows that our positive detections are not the result of a few discrepant points. We have also made a χ^2 analysis testing two hypotheses. We first test the hypothesis that our observations scatter normally around the instrumental polarization line (eq. [4]). The results are shown in Table 4, where we give the star and Julian Dates in columns (1) and (2), $\langle V \rangle \pm \sigma$ in column (3), and χ^2/ν and the number of degrees of freedom in column (4). We then test the hypothesis that a magnetic field has been detected with a fit of

$$\Delta V(t) = (-1)^w [V(t) - P(t)], \tag{5}$$

where $P(t)$ is given by equation (4), $w = 1$ for the blue-wing observations, and $w = 2$ for the red-wing observations. The χ^2/ν and ν values for this fit are shown

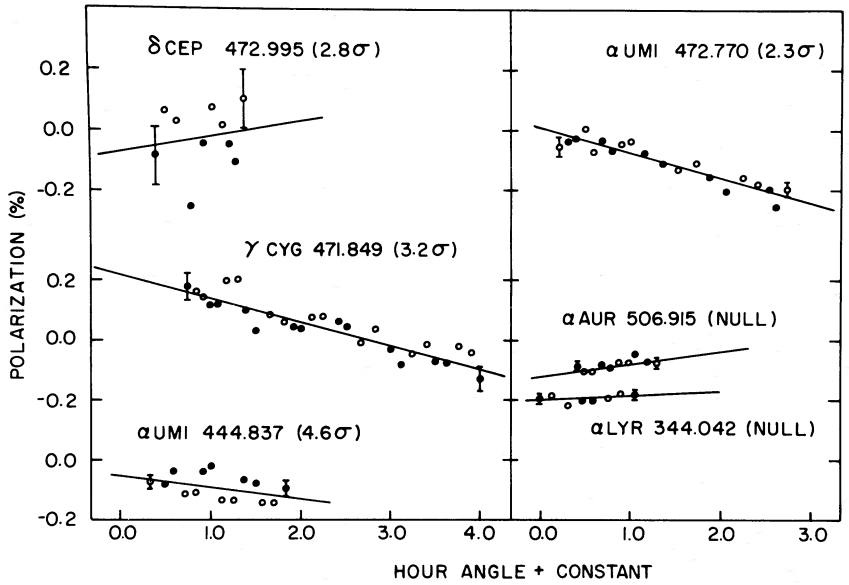

FIG. 2.—Individual polarization measurements are plotted as a function of hour angle (+ constant) for a few observations. They are identified with the name of the star, the Julian Date (−2,444,000), and the level of detection. *Open circles*, observations on the red wings of the lines; *filled circles*, observations on the blue wings; *full lines*, the least-squares fitted instrumental polarization. Representative error bars ($\pm\ \sigma$) are shown for selected points.

TABLE 4

χ^2 ANALYSIS

Star	JD (2,444,000+)	$\langle V\rangle \pm \sigma$ (%)	$\chi^2/\nu,(\nu)$ Equation (4)	$\chi^2/\nu,(\nu)$ Equation (5)	Remarks
δ Cep	472.995	−0.085±0.030	1.483 (8)	0.544 (7)	2.8 σ; Fig. 2
δ Cep	473.754	−0.026±0.011	1.010 (12)	0.58 (11)	2.4 σ
γ Cyg	444.775	0.000±0.009	0.284 (4)	0.378 (3)	null
γ Cyg	471.849	−0.029±0.009	0.854 (26)	0.435 (25)	3.2 σ; Fig. 2
γ Cyg	472.902	−0.015±0.0064	1.643 (16)	1.368 (15)	2.3 σ
α UMi ...	408.812	−0.0104±0.0064	0.654 (14)	0.625 (13)	null
α UMi ...	442.829	−0.014±0.0084	0.718 (12)	0.714 (11)	null
α UMi ...	444.837	0.031±0.0067	2.495 (12)	0.720 (11)	4.6 σ; Fig. 2
α UMi ...	470.984	−0.005±0.0065	1.675 (16)	1.740 (15)	null
α UMi ...	471.744	−0.007±0.0096	0.586 (10)	0.584 (9)	null
α UMi ...	472.770	−0.013±0.0057	1.178 (18)	0.964 (17)	2.3 σ; Fig. 2
α UMi ...	473.861	−0.014±0.0067	1.306 (14)	1.06 (13)	2.1 σ
α Lyr	344.042	0.001±0.006	0.116 (4)	0.145 (3)	Table 3; Fig. 2
α Lyr	507.638	0.0005±0.003	0.684 (6)	0.808 (5)	Table 3
α Aur	506.915	0.002±0.004	1.472 (8)	1.401 (7)	Table 3; Fig. 2

in column (5). Table 4 shows a large number of χ^2/ν values ≥ 1.0 in column (4) that indicate too large a scatter around the instrumental polarization line. On the other hand, column (5) shows that these χ^2/ν values are usually reduced to $\chi^2/\nu \leq 1.0$ when equation (5) is used. This shows, as seen in Figure 2, that the scatter is actually systematic, the observations on the blue wings having the tendency to lie on one side of the instrumental polarization line and the observations on the red wings on the other side. Particularly impressive is the decrease from 2.495 to 0.720 for the observation of αUMi having a detection at the 4.6 σ level. Three observations in Table 4 still have χ^2/ν values significantly larger than 1.0. They are: γ Cyg, JD=2,444,472.902, with $\chi^2/\nu=1.368$ and associated probability to exceed χ^2/ν $P(\chi^2,\nu)=0.15$; α UMi, JD=2,444,470.984 with $\chi^2/\nu=1.740$ and $P(\chi^2,\nu)=0.04$; α Aur, JD=2,444,506.915 with $\chi^2/\nu=1.401$ and $P(\chi^2,\nu)=0.20$. However, consider that we tested 15 observations and expected, therefore, 2.25 with $P(\chi^2,\nu)>0.15$ and 0.6

with $P(\chi^2, \nu) > 0.04$, essentially as seen in Table 4. Notice also that our χ^2 test actually tests two hypotheses simultaneously, that the errors are normally distributed and also that the instrumental polarization $P(t)$ varies linearly with time. The linear form of $P(t)$ is only an approximation that seems reasonable, and not rigorous, for the hour angles at which our observations were taken [see Borra 1976 for the actual $P(t)$], so this contributes in some measure to increase χ^2/ν.

In conclusion, a detailed consideration of our errors shows that we did not underestimate significantly our formal errors and that our observations behave as expected from low signal-to-noise measurements of the Zeeman effect.

It is of interest to examine the correlation between B_e and the phase of light variation. Unfortunately, we have only a few marginal detections, and correlations are thus difficult to see. For δ Cep, B_e is always negative, and the observations are compatible with a negative extremum occurring near the phase of maximum light [$\phi(B_{\min}) = 0.87$]. For αUMi, we see a lack of correlation with phase as the two detections near phase 0.9 show opposite polarities. On physical grounds, we would expect that B_e be modulated by two different periods, pulsational and rotational. These two observations of αUMi were taken at 28 days from each other so that the lack of correlation can be understood in terms of a period of rotation of a few tens of days. In this respect, it is satisfying to see that, in Table 2, observations taken on consecutive days are compatible with each other, within the errors. On the other hand, if the magnetic geometry is complex, a small change in the geometry can result in a change of polarity for B_e.

V. DISCUSSION AND CONCLUSIONS

Our instrument measures circular polarization; hence, we observe only the average longitudinal component of the magnetic field B_e that is defined by equation (3). Because B_e is highly dependent on the geometry of the magnetic field, it is difficult to estimate the ratio of effective field to surface field $r = B_e/B_s$ where B_s is defined by

$$B_s = \frac{\int |B| I \, dA}{\int I \, dA}. \tag{6}$$

For a dipolar field seen pole-on, $r = 0.4$, and it decreases to 0.0 as the dipole is tilted to the equator-on position. Therefore, the B_s values of δ Cep, α UMi, and γ Cyg are at least of the order of several tens of gauss but could be significantly larger for more complex geometries. If it is sufficiently strong, a surface magnetic field can be detected by the broadening it causes of the spectral lines. At a wavelength of 4200 Å and for $z = 1.3$, a magnetic field having $B_s = 2.3$ kilogauss introduces a broadening corresponding to 1 km s^{-1}. Cepheids and supergiants have large, microturbulent, velocity parameters V_m (Kraft 1960), typically $V_m \approx 5$ km s^{-1}. Therefore, a field having B_s of the order of 10^3 gauss could be hidden under the microturbulence and perhaps actually be responsible for a large part of the broadening that is classically interpreted as being due to microturbulence. Therefore, our observations are fully compatible with a tangled geometry having a B_s of the order of a kilogauss as assumed by Stothers (1979). If B_s contributes significantly to line broadening (and therefore to V_m), it could be detected because V_m, the equivalent widths, and the half-widths of spectral lines should correlate with their Zeeman structure and $z\lambda^2$. It is also tempting to speculate that the increase of V_m seen near minimum radius (Van Paradijs 1972) is caused in large part by an increase in B_s. Simple flux conservation arguments predict that $B_s \propto (1/r^2)$ and therefore that it should be maximum at minimum radius.

The discovery of magnetic fields in Cepheids and supergiants has many interesting astrophysical implications. The reconciliation between evolutionary and pulsational masses (Stothers 1979) has already been mentioned. Another important effect comes from the fact that the depth dependence of the ratio of magnetic to thermal pressures changes the period of pulsation for a given mass (Stothers 1979). This could be the elusive fourth parameter of the period-color-luminosity relation (Sandage 1972). Cepheids are important stepping stones in the determination of the extragalactic distance scale (Sandage and Tammann 1974). If, for whatever reason, the Cepheids used to calibrate the distances to M33 and NGC 2403 have abnormal magnetic structures, the justification for the extrapolation of the H II region diameter versus luminosity class to M101 will disappear, as the relation would then be accidental. This, in turn, will introduce an error in H_0 and q_0 (Sandage and Tammann 1975). If Cepheids and supergiants are magnetic, it is legitimate to wonder whether other pulsating variables and giants are also magnetic. Stothers (1979) finds a small shift of the blue edge of the instability strip for his Cepheid models. The blue edge of the instability strip of RR Lyrae variables is used to determine the helium abundance in those Population II stars (Tuggle and Iben 1972) and has important bearings on the primeval abundance of helium. Both a theoretical investigation of the effects of a magnetic field on the instability strip of RR Lyrae stars and an observational search for magnetic fields in RR Lyrae stars are thus in order. Hubbard and Dearborn (1980) find that the effect caused by a magnetic field could provide the necessary mixing to reduce the high C^{12}/C^{13}, predicted by stellar evolution models, to the lower, observed values. Their hypothesis is supported by our observations as they imply that many giants might be magnetic.

Finally, it is of interest to examine whether the present and previous claims of discoveries of magnetic fields in Cepheids and supergiants are compatible and mutually reinforcing. Weiss, Dorfi, and Tscharnuter (1980) and Weiss and Wood (1975) claim longitudinal magnetic fields of a few hundred gauss in four Cepheids, an order of magnitude larger than our detections. We have observed only one Cepheid (η Aql) contained in their list, but we do not detect a magnetic field, notwithstanding the fact that our errors (Table 2) are an order of magnitude smaller than theirs. It is possible that η Aql happened to have a smaller magnetic field at the time of our observations and that W Sgr, κ Pav, and β Dor have magnetic fields larger than the stars in our sample. However, this hypothesis is unlikely in view of the lack of detections in our extended list of fainter stars (Table 2). Our detections in γ Cyg are also considerably lower than the values claimed by Severny (1970) and all but one of the detections in Borra and Landstreet (1973). On the other hand, it is strange that so many detections are reported for that particular star.

We wish to thank Drs. N. R. Evans and D. G. Turner for useful conversations. One of us (E. F. B.) wishes to thank the Director of the Dominion Astrophysical Observatory, Dr. S. Van den Bergh, for the hospitality extended at the beginning of this investigation, and the Director of the Physics Department of Laval University, Prof. G. Nadeau, for liberating him from part of his academic duties at a crucial moment. Part of this research has been financed by a National Sciences and Engineering Research Council of Canada grant to E. F. B.

REFERENCES

Babcock, H. W. 1953, *Ap. J.*, **118**, 387.
_____. 1962, in *Astronomical Techniques*, ed. W. A. Hiltner (Chicago: University of Chicago Press), Chap. 5.
Borra, E. F. 1972, Ph.D. thesis, University of Western Ontario.
_____. 1974, *Ap. J.*, **188**, 287.
_____. 1976, *Pub. A.S.P.*, **88**, 548.
_____. 1981, *Pub. Vat. Obs.*, in press.
Borra, E. F., and Landstreet, J. D. 1973, *Ap. J.* (*Letters*), **185**, L139.
_____. 1980, *Ap. J. Suppl.*, **42**, 421.
Borra, E. F., and Vaughan, A. H. 1977, *Ap. J.*, **216**, 462.
Griffin, R. F., and Gunn, J. E. 1974, *Ap. J.*, **191**, 545.
Howard, R. 1977, *Ann. Rev. Astr. Ap.*, **15**, 153.
Hubbard, E. N., and Dearborn, D. S. P. 1980, *Ap. J.*, **239**, 248.
Kraft, R. P. 1960, in *Stellar Atmospheres*, ed. J. L. Greenstein (Chicago: University of Chicago Press), Chap. 9.
McClure, R. D., Fletcher, J. M., and Nemec, J. M. 1980, *Ap. J.* (*Letters*), **238**, L35.
Richardson, E. H., Brealey, G. A., and Dancey, R. 1971, *Pub. Dom. Ap. Obs. Victoria*, Vol. **14**, No 1.
Sandage, A. R. 1972, *Quart. J. R.A.S.*, **13**, 202.
Sandage, A. R. and Tammann, G. 1974, *Ap. J.*, **191**, 603.
_____. 1975, *Ap. J.*, **197**, 265.
Schaltenbrand, R., and Tammann, G. 1971, *Astr. Ap. Suppl.*, **4**, 265.
Severny, A. B. 1970, *Ap. J.* (*Letters*), **159**, L73.
Stothers, R. 1979, *Ap. J.*, **234**, 257.
Tuggle, R. S., and Iben, I. 1972, *Ap. J.*, **178**, 441.
Van Paradijs, J. 1972, *Nature Phys. Sci.*, **238**, 37.
Weiss, W. W., Dorfi, E., and Tscharnuter, W. M. 1980, preprint.
Weiss, W. W., and Wood, H. J. 1975, *Astr. Ap.*, **41**, 165.
Wood, H. J., Weiss, W. W., and Jenkner, H. 1977, *Astr. Ap.*, **61**, 181.
Wolff, S. C., and Bonsack, W. K. 1972, *Ap. J.*, **176**, 425.
Wolff, S. C., and Wolff, R. J. 1970, *Ap. J.*, **160**, 1049.

E. F. BORRA: Département de physique, Faculté des Sciences et de Génie, Université Laval, Québec, Canada G1K 7P4

J. M. FLETCHER and R. POECKERT: Dominion Astrophysical Observatory, 5071 West Saanich Road, Victoria, B. C., Canada V8X 3X3